

Electrophysiological Evidence for a Sensory Recruitment Model of Somatosensory Working Memory

Tobias Katus, Anna Grubert and Martin Eimer

Department of Psychology, Birkbeck College, University of London, London WC1E 7HX, UK

Address correspondence to Tobias Katus, Department of Psychological Sciences, Birkbeck College, University of London, Malet Street, London WC1E 7HX, UK. Email: t.katus@bbk.ac.uk

Sensory recruitment models of working memory assume that information storage is mediated by the same cortical areas that are responsible for the perceptual processing of sensory signals. To test this assumption, we measured somatosensory event-related brain potentials (ERPs) during a tactile delayed match-to-sample task. Participants memorized a tactile sample set at one task-relevant hand to compare it with a subsequent test set on the same hand. During the retention period, a sustained negativity (tactile contralateral delay activity, tCDA) was elicited over primary somatosensory cortex contralateral to the relevant hand. The amplitude of this component increased with memory load and was sensitive to individual limitations in memory capacity, suggesting that the tCDA reflects the maintenance of tactile information in somatosensory working memory. The tCDA was preceded by a transient negativity (N2cc component) with a similar contralateral scalp distribution, which is likely to reflect selection of task-relevant tactile stimuli at the encoding stage. The temporal sequence of N2cc and tCDA components mirrors previous observations from ERP studies of working memory in vision. The finding that the sustained somatosensory delay period activity varies as a function of memory load supports a sensory recruitment model for spatial working memory in touch.

Keywords: electroencephalography, event-related potentials, selective attention, somatosensation, working memory

Introduction

Working memory (WM) is responsible for the active maintenance of information that is no longer perceptually present. Visual and tactile WM are both assumed to be based on distributed neural networks that include prefrontal cortex (PFC) and modality-specific perceptual areas. The activation of PFC during the maintenance of visual and tactile stimuli in WM is well established (Fuster and Alexander 1971; Curtis and D'Esposito 2003; Romo and Salinas 2003; Curtis et al. 2004; Postle 2005; Kostopoulos et al. 2007). Additionally, modality-specific visual (Supér et al. 2001; Harrison and Tong 2009) or somatosensory areas (e.g., Zhou and Fuster 1996; Kaas et al. 2013) show persistent activation during the retention of visual or tactile stimuli. Although the exact role of this delay-period activity in visual areas during WM maintenance and their link to selective visual attention are still debated (e.g., van Dijk et al. 2010; Lewis-Peacock et al. 2012; Postle et al. 2013), its existence has led to the “sensory recruitment” model of WM (Pasternak and Greenlee 2005; Postle 2006; D'Esposito 2007; Harrison and Tong 2009). This model postulates that perceptual brain regions, which are responsible for the sensory processing of visual or tactile stimuli, are also involved in WM storage. The sustained activation of perceptual areas might be particularly important when WM tasks require the maintenance

of detailed sensory information (e.g., Lee et al. 2013; see also Sreenivasan et al. 2014).

Support for the sensory recruitment model comes from event-related potential (ERP) studies of visual WM (e.g., Vogel et al. 2005; Vogel and Machizawa 2004). In these studies, bilateral sample displays were followed after a retention interval by test displays, and participants had to match sample and test objects on one side of these displays. A sustained negativity at posterior electrodes contralateral to the side of the memorized objects (contralateral delay activity, CDA) started 300 ms after sample onset and persisted throughout the retention interval. The fact that this CDA component is sensitive to manipulations of visual WM load and to individual differences in WM capacity strongly suggests that the CDA directly reflects the maintenance of visual information in WM. The contralateral nature and posterior scalp topography of the CDA is consistent with neural generators in extrastriate visual areas (McCollough et al. 2007), in line with the sensory recruitment model. The CDA is typically preceded by an N2pc component that emerges around 200 ms post-stimulus, has a similar posterior scalp topography (e.g., McCollough et al. 2007), and reflects the attentional selection and encoding of task-relevant objects in ventral visual cortex (Luck and Hillyard 1994; Eimer 1996).

While ERP markers of visual WM are well established, corresponding electrophysiological correlates of tactile WM have not yet been described. Here, we demonstrate the existence of two somatosensory ERP components that are elicited during the encoding and maintenance of tactile stimuli in WM, and both show modality-specific topographies over primary somatosensory cortex. We employed a task that was modeled on the delayed match-to-sample task used in earlier studies of visual WM (e.g., Vogel and Machizawa 2004; Vogel et al. 2005). On each trial, a set of tactile sample stimuli was followed after a 2000-ms retention period by tactile test stimuli. Sample and test stimuli were delivered simultaneously to both hands, but the memory task had to be performed for one of these hands only. Participants had to encode and maintain tactile sample stimuli on the currently task-relevant hand and to match them to subsequent test stimuli on the same relevant hand. On low-load trials, a single tactile stimulus had to be maintained and matched. On high-load trials, two tactile pulses had to be memorized.

Results revealed the existence of two somatosensory ERP components that have not yet been described in the literature on tactile attention and WM. During the retention interval, a sustained tactile contralateral delay activity (tCDA) emerged with a modality-specific scalp distribution over somatosensory areas. This tCDA component was sensitive to memory load and to individual differences in tactile WM capacity. It was preceded by a central contralateral negativity (N2cc component) with a similar modality-specific topography that was also

modulated by WM load. Analogous to the visual N2pc and CDA, these N2cc and tCDA components reflect the spatially selective encoding and maintenance of task-relevant information in tactile WM.

Materials and Methods

Participants

Eighteen neurologically unimpaired paid adult participants were tested. The study was conducted in accordance with the Declaration of Helsinki and was approved by the Psychology Ethics Committee, Birkbeck College. All participants gave informed written consent prior to testing. Two participants were excluded from analysis because their tactile WM capacity measured by Cowan's *K* (Cowan 2001) was below 1. Sixteen participants remained in the sample (mean age 32 years, range 25–44 years, 3 male, 13 right-handed).

Stimuli and Task Design

Participants were seated in a dimly lit recording chamber, viewing a monitor showing a central white fixation cross against a black background. Both hands were covered from sight and were placed on a table at a distance of approximately 40 cm. Eight mechanical tactile stimulators were attached to the distal phalanges of the index, middle, ring, and small fingers of the left and right hand. Stimulators were driven by an eight-channel sound card (M-Audio, Delta 1010LT) and custom-built amplifiers, controlled by Matlab (MathWorks). Continuous white noise was delivered via headphones to mask sounds produced by the tactile stimulators. All tactile stimuli were 100-Hz sinusoids (duration: 200 ms; intensity: 0.37 N).

Figure 1 illustrates the experimental procedure. Each trial started with a set of tactile sample stimuli that were delivered simultaneously to the left and right hand. After a 2000-ms retention period, a set of tactile test stimuli was presented simultaneously to both hands. Prior to the start of each block, instructions displayed on the monitor informed participants whether the left or right hand was relevant in the upcoming block. Participants had to decide whether sample and test stimulus locations on this hand were identical (match trials) or different (mismatch trials). The task-relevant hand was swapped after each experimental block. Two load conditions were randomized within each block. In the "low-load condition," one sample pulse was presented with equal probability to one of the four fingers of the left hand and the right hand. On match trials, the test pulse was delivered to the same finger of the relevant hand as the sample pulse. On mismatch trials, one of the three other fingers on that hand was stimulated at test. In the "high-load condition," two sample pulses were presented to two randomly selected fingers of the left hand and the right hand,

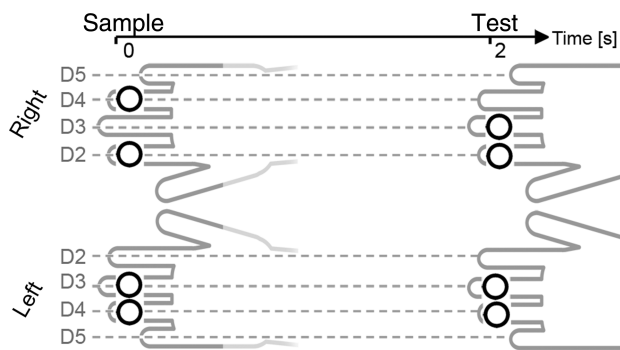


Figure 1. Illustration of the experimental setup. Participants memorized a tactile sample set at one task-relevant hand to compare it with a test set on the same hand after a 2-s retention period. Memory load was varied between trials (low load: one pulse, high load: two pulses per hand). The relevant hand (left, right) was varied between blocks. The example shown here illustrates a high-load trial where the locations of tactile sample and test stimuli (symbolized by white dots) are identical at the left hand (match), but not at the right hand (mismatch).

respectively. On match trials, test pulses were delivered to the same two fingers of the relevant hand. On mismatch trials, at least one of the two test pulses was presented to a different finger of that hand. Because one of the two sample locations could be repeated at test on mismatch trials, participants had to retain the location of both sample stimuli on the relevant hand to perform the task in the high-load condition. Match and mismatch trials were equiprobable. On the currently task-irrelevant hand, sample and test stimuli were also presented at matching or mismatching locations, and this was independent of whether there was a match or mismatch on the relevant hand.

Participants signaled a match or mismatch between sample and test on the relevant hand with a vocal response ("a" for match and "e" for mismatch) that was recorded with a headset microphone between 200 and 1700 ms after test stimulus offset. A question mark replaced the fixation cross on the monitor during this period. The interval between the offset of this question mark and the onset of the sample pulses on the next trial varied between 800 and 1100 ms. The experiment included ten blocks of 48 trials, with twelve trials per block for each of the four combinations of high- versus low-load trials and match versus mismatch trials. Instructions emphasized accuracy over speed, and the need to avoid head and arm movements and to maintain central gaze fixation. Feedback on hit and correct rejection rates was provided after each block. Two training blocks were run prior to the first experimental block.

Processing of EEG Data

Electroencephalography (EEG) data, sampled at 500 Hz using a Brain-Vision amplifier, were DC-recorded from 64 Ag/AgCl active electrodes at standard locations of the international 10–10 system. Two electrodes at the outer canthi of the eyes monitored lateral eye movements (horizontal electro-oculogram, HEOG), and electrodes sites TP9/10 were used as mastoid references. Continuous EEG data were referenced to the left mastoid during recording and were offline re-referenced to the arithmetic mean of both mastoids and submitted to a 40-Hz low-pass finite impulse response filter (Blackman window, filter order 666). EEG epochs for the 2000-ms interval following sample stimulus onset were computed relative to a 200-ms pre-stimulus baseline. Blind source separation of EEG data was performed with the Independent Component Analysis (ICA) algorithm implemented in the EEGLab toolbox (Delorme and Makeig 2004; Delorme et al. 2007). Independent components related to artifacts at anterior scalp regions (in particular, eye movements and blinks) were identified by visual inspection and subtracted from the EEG data. To obtain reliable ICA decompositions, a copy of the data was segmented into eight 250-ms frames covering the 2000-ms retention period. These frames were corrected using whole-epoch baselines to achieve data stationarity (cf., Groppe et al. 2009) without high-pass filtering, which would have removed slow brain potentials. The copy was discarded after ICA decompositions had been applied to the original data set. Epochs with lateral eye movements that escaped ICA artifact correction were identified and removed with a differential step function on the bipolarized HEOG (step width 100 ms, threshold 24 μ V). The resulting HEOG waveforms contained no systematic eye gaze deflections toward the task-relevant hand (Fig. 2, bottom panel). After artifact rejection and elimination of trials with incorrect responses, 90.2% of all epochs were retained for statistical analyses (low load: 93.4%; high load: 87.1%).

Results

Behavioral Performance

Participants responded correctly on 97.1% of all low-load trials and 90.4% of all high-load trials. Sensitivity indices (d') were analyzed in a two-way repeated-measures ANOVA with the factors memory load (low and high) and relevant hand (left and right). Performance was reduced with high load relative to low load ($F_{1,15} = 71.728$, $P < 10^{-6}$) and did not differ between blocks where the left or right hand was relevant ($F_{1,15} = 1.081$, $P > 0.3$). A significant memory load \times relevant hand interaction ($F_{1,15} = 6.222$, $P = 0.025$) was due to the fact that the

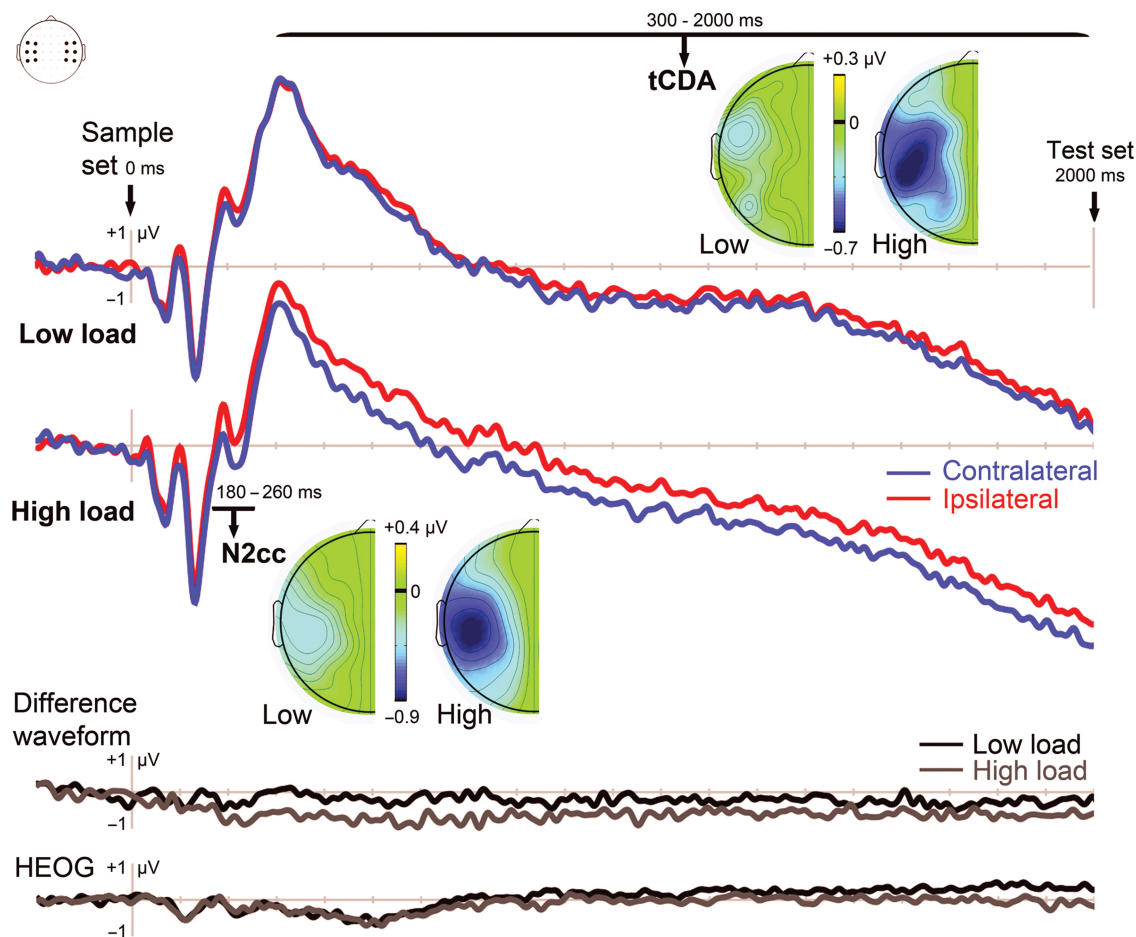


Figure 2. Grand mean ERPs elicited in the 2000-ms interval following sample stimulus onset in the low-load and high-load conditions. ERPs were averaged across lateral central electrode clusters contralateral (blue lines) and ipsilateral (red lines) to the hand where the memory task was performed. Difference maps show the topographical distribution of lateralized effects in the N2cc (bottom) and tCDA (top) time windows. These maps represent the amplitude difference of contralateral minus ipsilateral recordings, collapsed across blocks where the memory task was performed with the left or right hand. Enhanced contralateral negativities are shown in blue. The two bottom panels show difference waveforms for the low-load and high-load condition, obtained by subtracting electrodes ipsilateral to the task-relevant hand from contralateral electrodes, and HEOG difference waveforms, calculated by subtracting HEOG electrodes ipsilateral to the task-relevant hand from contralateral electrodes after artifact rejection. In these HEOG difference waves, any eye movements toward the task-relevant hand would be reflected by negative (downward) HEOG deflections.

performance decrement with high as compared with low memory load was larger when the memory task was performed with the left hand (8.5%) relative to blocks where the right hand was relevant (4.9%).

Mean vocal reaction times (RTs) in trials with correct responses were faster in the low-load relative to the high-load condition (799 ms vs. 817 ms; main effect of memory load: $F_{1,15} = 8.801$, $P = 0.010$). RTs did not differ between blocks where the left or right hand was task-relevant ($F_{1,15} = 1.846$, $P > 0.1$). The memory load \times relevant hand interaction was significant ($F_{1,15} = 5.25$, $P = 0.037$), as the RT costs for the low-load versus high-load condition were larger when the memory task was performed with the right hand (26 ms) relative to blocks where the left hand was relevant (10 ms). In other words, there was an asymmetric speed-accuracy tradeoff between the two hands for task performance in the high-load versus low-load condition.

Electrophysiological Data

Figure 2 shows ERP waveforms averaged across lateral central electrodes (FC3/4, FC5/6, C3/4, C5/6, CP3/4, and CP5/6)

contralateral and ipsilateral to the task-relevant hand for the 2000-ms interval between the bilateral sample stimulus and the subsequent test stimulus. Results are shown separately for the low-load and high-load conditions. Following the early sensory-evoked ERP components to the sample stimulus, ERP waveforms were characterized by a gradually developing sustained negativity that reached its maximal amplitude immediately before the onset of the test stimuli. This sustained negativity that was present at contralateral as well as ipsilateral electrodes reflects the Contingent Negative Variation (CNV; see Birbaumer et al. 1990) that is elicited in anticipation of expected task-relevant events such as the test stimulus set used in this study. More importantly, sample stimuli triggered a transient enhanced negativity contralateral to the task-relevant hand. This N2cc component emerged around 180 ms after sample stimulus onset, and its amplitude was larger in the high-load as compared with the low-load condition. The N2cc was followed by a sustained contralateral negativity (tCDA) that remained present throughout the retention period. This tCDA component was larger when two stimuli rather than one tactile stimulus had to be memorized. The topographical maps in Figure 2 illustrate the scalp distribution of N2cc and tCDA components

in the low-load and high-load conditions. Data shown in these maps were collapsed across blocks where the left or right hand was task-relevant by flipping ERPs at contralateral electrodes in blocks with a left-hand memory task over the midline. Both N2cc and tCDA components were maximal over somatosensory areas in the post-central gyrus and adjacent parietal regions (see also Fig. 4).

Difference waveforms were computed by subtracting ERPs ipsilateral to the currently task-relevant hand from contralateral ERPs. Statistical tests were conducted on mean amplitudes of these difference waves for a time window centered on the N2cc component (180–260 ms post-stimulus) and a second window centered on the tCDA (300–2000 ms). Difference values that statistically differ from zero mark the presence of lateralized components in the ERP waveforms. The N2cc was present in both the low-load ($t_{15} = -5.593$, $P < 10^{-4}$) and high-load condition ($t_{15} = -7.037$, $P < 10^{-5}$). N2cc amplitudes were significantly larger with high relative to low memory load ($t_{15} = 4.235$, $P < 10^{-3}$). The tCDA component was present with low load ($t_{15} = -2.951$, $P = 0.010$) as well as with high memory load ($t_{15} = -6.126$, $P < 10^{-4}$). Similar to the N2cc, tCDA amplitudes were significantly larger in the high-load relative to the low-load condition ($t_{15} = 3.801$, $P = 0.002$).

An additional analysis of mean amplitudes in the tCDA time window obtained for the unsubtracted ERP waveforms revealed a main effect of contralaterality (electrodes contralateral vs. ipsilateral to the task-relevant hand; $F_{1,15} = 38.006$, $P < 10^{-4}$) that interacted with load ($F_{1,15} = 14.448$, $P = 0.002$), due to the fact that the tCDA was larger in the high-load condition. There was also a main effect of load ($F_{1,15} = 14.862$, $P = 0.002$), with larger CNV components with high memory load. This load-dependent modulation of CNV amplitudes was reliable at contralateral as well as ipsilateral electrodes ($t_{15} = -4.500$ and -2.481 , $P < 0.001$ and 0.026 , respectively).

Tactile WM capacity was calculated for each individual participant on the basis of their performance in the high-load condition, using the formula $K = (\text{hits} + \text{correct rejections} - 1) \times 2$, where 2 is memory set size in this condition (Cowan 2001). As illustrated in Figure 3, individual memory capacity was reliably correlated with the difference of tCDA amplitudes between the high-load and low-load conditions ($r = -0.640$, $P = 0.008$).

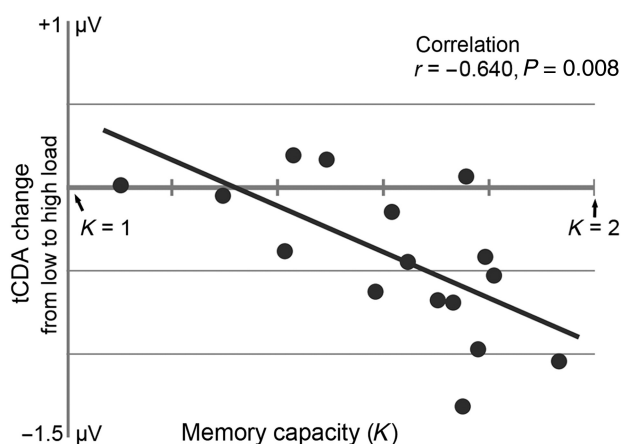


Figure 3. Correlation of individual participant's tactile WM capacity K (x -axis) and the increase of tCDA amplitudes in the high-load relative to the low-load condition measured for each participant (y -axis). K was calculated on the basis of individual performance in the high-load condition.

Participants with higher tactile WM capacity showed a more pronounced increase of the tCDA component on trials with high versus low memory load than participants with lower capacity. No correlation was found between individual K values and the difference of N2cc amplitudes between high- and low-load conditions ($P > 0.7$).

To obtain additional evidence for a link between tCDA amplitudes and behavioral performance at the level of individual trials in the high-load condition, we computed tCDA components in the high-load condition separately for trials with vocal RTs above and below the median RT (with RT median splits conducted individually for each participant and trial condition). Trials with fast responses were more accurate than slow response trials (Cowan's K : fast = 1.786, slow = 1.453; $t_{15} = 6.362$, $P < 10^{-4}$). Critically, tCDA amplitudes were larger for fast as compared with slow response trials (-0.749 vs. -0.594 μV), and this amplitude difference was significant ($t_{15} = -2.564$, $P = 0.022$).

An additional current source density (CSD) analysis was conducted to further illustrate the modality-specific scalp topographies of the N2cc and tCDA components and to demonstrate that the selection of lateral central electrodes for the analysis of these components was appropriate. ERP data were collapsed across the low- and high-load conditions, after conversion of scalp potentials to surface Laplacians ($\lambda = 10^{-5}$, iterations = 50, $m = 4$; cf. Tenke and Kayser 2012). This transformation minimizes the effects of volume conduction from remote sources and leads to a reference-independent representation of EEG/ERP data. CSD topographies provide a conservative estimate of the neural generator patterns that contribute to scalp-recorded ERPs (Nunez and Westdorp 1994; Tenke and Kayser 2012). Robust lateralized effects were found over somatosensory brain regions (Fig. 4), as demonstrated by significant differences of contra- minus ipsilateral activity recorded at central electrodes in the time window of N2cc ($t_{15} = -6.476$, $P < 10^{-4}$) and tCDA ($t_{15} = -4.066$, $P = 0.001$). Apart from an almost significant contralateral positivity at anterior regions during the N2cc time window ($t_{15} = 2.107$, $P = 0.052$), no statistically reliable

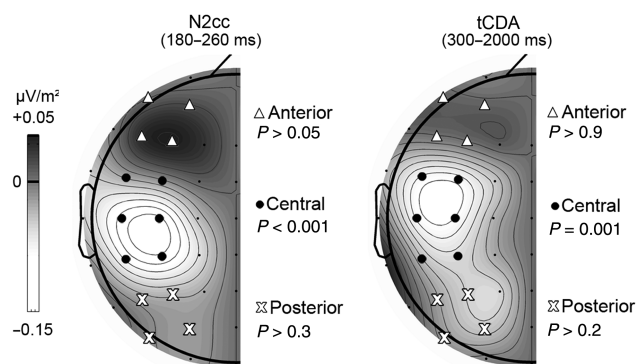


Figure 4. Grand mean CSD topographical maps, showing the scalp distribution of lateralized effects in the N2cc and tCDA time windows. These maps represent the amplitude difference of contralateral minus ipsilateral recordings, collapsed across blocks where the memory task was performed with the left or right hand, and averaged across the low- and high-load conditions. Six electrodes at lateral central scalp regions (black dots) were averaged for each recording cluster (contra- and ipsilateral to the task-relevant hand). The presence of lateralized effects was also tested for different sets of electrodes over anterior (white triangles) and posterior (white crosses) scalp areas. Reliable lateralized effects were present only for the central electrode cluster.

lateralization was evident over posterior (electrodes P3/4, P5/6, PO3/4, and PO7/8) and anterior (electrodes AF3/4, AF7/8, F3/4, and F5/6) scalp regions (all P s > 0.2; see Fig. 4).

Discussion

We employed a tactile memory task that was modeled on the delayed match-to-sample task used in previous research on visual WM (e.g., Vogel and Machizawa 2004) to identify ERP correlates of the selection and maintenance of task-relevant tactile stimuli. When participants memorized the spatial locations of one or two tactile sample pulses on the left or the right hand, an enhanced negativity with a centroparietal focus emerged contralateral to the hand where the memorized tactile sample was delivered. This tCDA component was sensitive to tactile WM load, as it was larger on trials where participants had to remember two tactile stimulus locations than when only a single tactile location had to be memorized (Fig. 2). The load-dependent increase of tCDA amplitudes was more pronounced for participants with higher tactile WM capacity than for individuals whose capacity (measured by Cowan's K) was closer to 1 (Fig. 3), mirroring previous findings for the visual CDA component (Vogel and Machizawa 2004). Furthermore, the tCDA component was reliably larger on trials with fast vocal responses in the high-load condition, which were also more accurate than slow responses. This demonstrates that the tCDA component is linked to behavioral performance on individual trials. These observations strongly suggest that the tCDA is an electrophysiological correlate of the maintenance of somatosensory information in tactile WM.

Analogous to the visual CDA, which has a modality-specific topography over posterior visual cortex (McCollough et al. 2007), the tactile CDA component emerged at contralateral central electrodes. The scalp topography of the tCDA in a CSD-transformed map (Fig. 4) also suggests neural generators that are located within the somatosensory system. We conclude that the tCDA component reflects the spatially selective activation of modality-specific brain regions contralateral to the task-relevant hand during the retention of tactile stimuli in WM. These results provide new support for the sensory recruitment model, which assumes that brain regions involved in the perceptual processing of sensory stimuli are also active during the maintenance of these stimuli in WM. It should be noted that topographical distributions of CSD-transformed scalp maps only allow relatively coarse approximations of the neural origins of components such as the tCDA and that the exact anatomical basis of this component needs to be determined in future work.

Previous research has used transcranial magnetic stimulation (TMS; Harris et al. 2002) and EEG source reconstruction techniques in studies with human participants (Spitzer and Blankenburg 2011), as well as single-cell recordings in monkeys (Romo and Salinas 2003) to show that the activity of neurons in primary (SI) and secondary (SII) somatosensory cortex is modulated in tactile WM tasks. For example, a suppression of alpha activity indicative of attentional processing was found over contralateral SI during the retention period of a vibrotactile frequency discrimination task (Spitzer and Blankenburg 2011). Asymmetric alpha-band oscillations have also been suggested as the physiological basis of the visual CDA component (van Dijk et al. 2010). Indirect evidence for a recruitment of somatosensory brain areas comes from a tactile

EEG study that used task-irrelevant probe stimuli presented during the retention period to examine how WM influences somatosensory encoding (Katus et al. 2012). The retention of locations in WM was mirrored by spatially selective modulation of early ERP components to tactile probe stimuli with putative origins in somatosensory areas such as SII (Frot and Mauguière 1999). These lines of evidence point toward close links between the maintenance of tactile information in WM and the spatially specific activation of early somatosensory areas. The critical new finding of the present study is the discovery of the tCDA component that reflects the maintenance of tactile information in a sustained and load-dependent manner. Because the tCDA is computed by comparing ERPs at electrodes contralateral and ipsilateral to the location of memorized tactile events, it only reflects the difference in the absolute activation of contralateral versus ipsilateral somatosensory areas and should therefore not be interpreted as evidence that tactile WM storage is exclusively contralateral. In fact, there is electrophysiological evidence that ipsilateral somatosensory cortex may also be involved in the maintenance of tactile pattern information (Li Hegner et al. 2007).

The tCDA component was preceded by an earlier contralateral negativity (N2cc component), which emerged around 180 ms after sample stimulus onset. Similar to the tCDA, the N2cc showed a centroparietal scalp topography (see Figs 2 and 4) and was larger in the high-load as compared with the low-load condition. This new N2cc component is likely to represent the somatosensory equivalent of the well-known visual N2pc component. The N2pc is triggered at contralateral posterior electrodes at a similar post-stimulus latency during the attentional selection of targets among distractors in visual displays (Luck and Hillyard 1994; Eimer 1996) and precedes the CDA in visual WM studies that employ a similar delayed match-to-sample task as the one used in the present study (e.g., McCollough et al. 2007; Anderson et al. 2011). The load-dependent increase of the tactile N2cc component observed in the present study mirrors previous findings for the visual N2pc, which increases in size with the number of attended objects in visual displays (e.g., Drew and Vogel 2008; Mazza and Caramazza 2011).

The absence of N2cc components in previous ERP studies of tactile spatial attention is due to the fact that instead of employing bilateral stimuli, tactile events were delivered to a single location on the left or right hand. In these studies, modality-specific components of the somatosensory event-related potential, such as the P100 or N140, were found to be larger for tactile stimuli at currently attended as compared with unattended positions (e.g., Forster and Eimer 2005), demonstrating that spatial attention enhances the sensory processing of tactile events. Analogous to the visual N2pc, which is elicited when target and distractor objects appear in both visual hemifields, measurement of the N2cc component requires that relevant and irrelevant tactile events are presented simultaneously to both hands, or to other homologous locations on the left and right side of the body. Note that the modality-specific somatosensory N2cc component found here is distinct from another ERP component with the same label that has been observed in stimulus-response compatibility experiments and is linked to visuospatially guided response selection (Praamstra and Oostenveld 2003). The question whether the effects of memory load on the N2cc and tCDA components reflect load-sensitive modulations of two distinct processing stages (i.e., the attentional selection and the subsequent storage of task-

relevant tactile information in WM) or of a single memory maintenance stage that temporally overlaps with the N2cc component needs to be investigated in future studies where the demands on attentional target selection and WM load are independently manipulated. In addition to the N2cc and tCDA components, a sustained bilateral CNV component that was observed in the interval between sample and test stimuli was also modulated by memory load. This modulation may primarily reflect differences in the preparation for the match/mismatch decision in response to the test stimulus, which is more demanding in the high-load condition. However, the presence of load effects at ipsilateral electrodes could in principle as well reflect contributions of ipsilateral somatosensory cortex to WM maintenance (Li Hegner et al. 2007; see also van Ede et al. 2014).

When considered together with the results of previous ERP investigations of visual WM (Vogel and Machizawa 2004; Vogel et al. 2005; McCollough et al. 2007; Anderson et al. 2011), the current findings reveal striking similarities between the mechanisms that underlie the spatial selection and selective maintenance of sensory stimuli in vision and touch. During both visual and tactile WM tasks, two contralateral ERP components are elicited successively, with a highly similar time course in both modalities. N2pc and N2cc components that emerge around 180 ms after sample display onset reflect spatial selection during encoding of task-relevant visual or tactile information. The subsequent CDA and tCDA components are linked to the sustained maintenance of stored information during the retention period. The fact that the load-sensitive tCDA component observed in this study showed a topography over lateral central somatosensory areas (see Fig. 4) whereas the visual CDA component is elicited over lateral posterior visual cortex (McCollough et al. 2007) strongly suggests that the maintenance of visual or tactile information in WM involves the activation of distinct modality-specific regions, in line with the sensory recruitment model of WM (Pasternak and Greenlee 2005; Postle 2006; D'Esposito 2007; Sreenivasan et al. 2014). In both vision and touch, neural networks that mediate the perceptual processing of sensory signals contribute to the storage and maintenance of information in WM.

Funding

This work was funded by the Deutsche Forschungsgemeinschaft (DFG grant KA 3843/1-1), and was supported by a grant from the Economic and Social Research Council (ESRC), United Kingdom.

Notes

We thank Sue Nicholas for invaluable help in setting up the hardware used for tactile stimulation. *Conflict of Interest:* None declared.

References

Anderson DE, Vogel EK, Awh E. 2011. Precision in visual working memory reaches a stable plateau when individual item limits are exceeded. *J Neurosci.* 31(3):1128–1138.

Birbaumer N, Elbert T, Canavan AG, Rockstroh B. 1990. Slow potentials of the cerebral cortex and behavior. *Physiol Rev.* 70(1):1–41.

Cowan N. 2001. The magical number 4 in short-term memory: a reconsideration of mental storage capacity. *Behav Brain Sci.* 24(1): 87–114x.

Curtis CE, D'Esposito M. 2003. Persistent activity in the prefrontal cortex during working memory. *Trends Cogn Sci.* 7(9):415–423.

Curtis CE, Rao VY, D'Esposito M. 2004. Maintenance of spatial and motor codes during oculomotor delayed response tasks. *J Neurosci.* 24(16):3944–3952.

Delorme A, Makeig S. 2004. EEGLAB: an open source toolbox for analysis of single-trial EEG dynamics including independent component analysis. *J Neurosci Methods.* 134(1):9–21.

Delorme A, Sejnowski T, Makeig S. 2007. Enhanced detection of artifacts in EEG data using higher-order statistics and independent component analysis. *Neuroimage.* 34(4):1443–1449.

D'Esposito M. 2007. From cognitive to neural models of working memory. *Philos Trans R Soc Lond B Biol Sci.* 362(1481):761–772.

Drew T, Vogel EK. 2008. Neural measures of individual differences in selecting and tracking multiple moving objects. *J Neurosci.* 28(16): 4183–4191.

Eimer M. 1996. The N2pc component as an indicator of attentional selectivity. *Electroencephalogr Clin Neurophysiol.* 99(3):225–234.

Forster B, Eimer M. 2005. Covert attention in touch: Behavioral and ERP evidence for costs and benefits. *Psychophysiology.* 42(2):171–179.

Frot M, Mauguière F. 1999. Timing and spatial distribution of somatosensory responses recorded in the upper bank of the sylvian fissure (SII area) in humans. *Cereb Cortex.* 9(8):854–863.

Fuster JM, Alexander GE. 1971. Neuron activity related to short-term memory. *Science.* 173(3997):652–654.

Groppe DM, Makeig S, Kutas M. 2009. Identifying reliable independent components via split-half comparisons. *Neuroimage.* 45(4):1199–1211.

Harris JA, Miniussi C, Harris IM, Diamond ME. 2002. Transient storage of a tactile memory trace in primary somatosensory cortex. *J Neurosci.* 22(19):8720–8725.

Harrison SA, Tong F. 2009. Decoding reveals the contents of visual working memory in early visual areas. *Nature.* 458(7238):632–635.

Kaas AL, van Mier H, Visser M, Goebel R. 2013. The neural substrate for working memory of tactile surface texture. *Hum Brain Mapp.* 34(5):1148–1162.

Katus T, Andersen SK, Müller MM. 2012. Maintenance of tactile short-term memory for locations is mediated by spatial attention. *Biol Psychol.* 89(1):39–46.

Kostopoulos P, Albanese M, Petrides M. 2007. Ventrolateral prefrontal cortex and tactile memory disambiguation in the human brain. *Proc Natl Acad Sci USA.* 104(24):10223–10228.

Lee SH, Kravitz DJ, Baker CI. 2013. Goal-dependent dissociation of visual and prefrontal cortices during working memory. *Nature Neurosci.* 16(8):997–999.

Lewis-Peacock JA, Drysdale AT, Oberauer K, Postle BR. 2012. Neural evidence for a distinction between short-term memory and the focus of attention. *J Cogn Neurosci.* 24(1):61–79.

Li Hegner Y, Lutzenberger W, Leiberg S, Braun C. 2007. The involvement of ipsilateral temporoparietal cortex in tactile pattern working memory as reflected in beta event-related desynchronization. *Neuroimage.* 37(4):1362–1370.

Luck SJ, Hillyard SA. 1994. Spatial filtering during visual search: evidence from human electrophysiology. *J Exp Psychol Hum Percept Perform.* 20(5):1000–1014.

Mazza V, Caramazza A. 2011. Temporal brain dynamics of multiple object processing: the flexibility of individuation. *PLoS ONE.* 6(2):e17453.

McCollough AW, Machizawa MG, Vogel EK. 2007. Electrophysiological measures of maintaining representations in visual working memory. *Cortex.* 43(1):77–94.

Nunez PL, Westdorp AF. 1994. The surface Laplacian, high resolution EEG and controversies. *Brain Topogr.* 6(3):221–226.

Pasternak T, Greenlee MW. 2005. Working memory in primate sensory systems. *Nat Rev Neurosci.* 6(2):97–107.

Postle BR. 2005. Delay-period activity in the prefrontal cortex: one function is sensory gating. *J Cogn Neurosci.* 17(11):1679–1690.

Postle BR. 2006. Working memory as an emergent property of the mind and brain. *Neuroscience.* 139(1):23–38.

Postle BR, Awh E, Serences JT, Sutterer DW, D'Esposito M. 2013. The positional-specificity effect reveals a passive-trace contribution to visual short-term memory. *PLoS ONE.* 8(12):e83483.

- Praamstra P, Oostenveld R. 2003. Attention and movement-related motor cortex activation: a high-density EEG study of spatial stimulus-response compatibility. *Brain Res Cogn Brain Res*. 16(3):309–322.
- Romo R, Salinas E. 2003. Flutter discrimination: neural codes, perception, memory and decision making. *Nat Rev Neurosci*. 4(3):203–218.
- Spitzer B, Blankenburg F. 2011. Stimulus-dependent EEG activity reflects internal updating of tactile working memory in humans. *Proc Natl Acad Sci USA*. 108(20):8444–8449.
- Sreenivasan KK, Curtis CE, D'Esposito M. 2014. Revisiting the role of persistent neural activity during working memory. *Trends Cogn Sci*. 18(2):82–89.
- Supér H, Spekreijse H, Lamme VA. 2001. A neural correlate of working memory in the monkey primary visual cortex. *Science*. 293(5527):120–124.
- Tenke CE, Kayser J. 2012. Generator localization by current source density (CSD): implications of volume conduction and field closure at intracranial and scalp resolutions. *Clin Neurophysiol*. 123(12):2328–2345.
- van Dijk H, van der Werf J, Mazaheri A, Medendorp WP, Jensen O. 2010. Modulations in oscillatory activity with amplitude asymmetry can produce cognitively relevant event-related responses. *Proc Natl Acad Sci USA*. 107(2):900–905.
- van Ede F, de Lange FP, Maris E. 2014. Anticipation increases tactile stimulus processing in the ipsilateral primary somatosensory cortex. *Cereb Cortex*. 24:2562–2571.
- Vogel EK, Machizawa MG. 2004. Neural activity predicts individual differences in visual working memory capacity. *Nature*. 428(6984):748–751.
- Vogel EK, McCollough AW, Machizawa MG. 2005. Neural measures reveal individual differences in controlling access to working memory. *Nature*. 438(7067):500–503.
- Zhou YD, Fuster JM. 1996. Mnemonic neuronal activity in somatosensory cortex. *Proc Natl Acad Sci USA*. 93(19):10533–10537.